Extension of the variational theory of complex rays to shells for medium-frequency vibrations

H. Riou, P. Ladevèze*, P. Rouch

LMT Cachan (ENS Cachan/CNRS/Paris 6 University), 61 avenue du President Wilson, 94235 Cachan Cedex, France

Received 9 May 2002; accepted 20 March 2003

Abstract

A new approach to the calculation of vibrations of weakly damped elastic structures in the medium-frequency range, called the *variational theory of complex rays* (VTCR), is being developed. Here, the extension of this theory to shells of relatively small curvature is considered. Numerical examples of structures made of plates and shells demonstrate the capabilities of the VTCR.
© 2003 Elsevier Ltd. All rights reserved.

1. Introduction

A key point in structural design is the modelling and calculation of the vibrational response of elastic structures. The low-frequency range no longer poses major difficulties, even for complex structures. For the high-frequency range, there are efficient computational tools which are quite distinct from those used for low frequencies, and particularly from the statistical energy analysis (SEA) method in which the spatial aspect disappears almost entirely [1–4].

However, the modelling and calculation of the vibrational response in the medium-frequency range, which is the topic of this paper, continue to create problems. The difficulty lies in the length of variation of the phenomena being studied, which is very small compared to characteristic dimension of the structure. Consequently, if one of the low-frequency methods were to be applied, apart from the serious numerical difficulties which are already present, the finite element calculation to be performed would require an unreasonable number of degrees of freedom (DOF). Nevertheless, much work is currently being done in order to extend the frequency range for these methods. A first result is that a pollution error affects the accuracy of the finite element solution [5–7]. Various enhanced finite element approaches have been studied [8–16].

---

*Corresponding author. Tel.: +33-1-47-402241; fax: +33-1-47-402785.
  E-mail address: ladeveze@lmt.ens-cachan.fr (P. Ladevèze).

Difficulties would also appear if one were to apply the SEA method, which is normally used for high frequencies.

There are few other works concerning the calculation of medium-frequency vibrations. For rods and beams, the problem is much easier and has been solved [17,18]. Very few works deal with complex structures, such as plates or shells [18–22]. These methods, which are closely related to finite element methods, propose reduced bases for the medium-frequency calculation obtained by a specific treatment in space or over the frequency bandwidth. In the authors' opinion, with the exception of the theory introduced in Ref. [23], these methods are not true medium-frequency methods because the phenomena associated with small variations of length, although not very significant, remain present. In other words, these methods do not strictly involve the effective quantities for the time and space scales considered and, therefore, give results which are very sensitive to data errors. The theory initiated in Ref. [23] is built upon the notions of effective energy density and effective vibrational energy. This heuristic theory is extremely attractive. However, despite the improvements already made [24–26], this theory still encounters some obstacles [27,28].

The alternative approach developed here is called the *variational theory of complex rays* (VTCR) and was introduced in Ref. [29]. It is a true medium-frequency method. The most fundamental aspects of this approach are described in Ref. [30].

The first feature which characterizes the VTCR is the use of a new variational formulation of the problem to be solved, which was developed in order to allow a priori independent approximations within the substructures (i.e. approximations which are not required a priori to verify the transmission conditions in terms of displacements and stresses at the interfaces between substructures). The transmission conditions are incorporated instead in the variational formulation.

The second feature characterizing the VTCR is the introduction of two-scale approximations with a strong mechanical meaning: the solution is assumed to be well-described locally in the neighbourhood of a point $\mathbf{X}$ as the superposition of an infinite number of local vibration modes. These basic modes (which can be interior modes, edge modes or corner modes) verify the laws of dynamics. All wave directions are taken into account; the unknowns are discretized amplitudes with relatively long wavelengths.

The last feature characterizing the VTCR is that only effective quantities related to the elastic energy, the kinetic energy, the dissipation work, the effective displacement, etc., are retained from the calculated discretized amplitudes.

For bars and beams, the VTCR leads to the exact solution. Results concerning plates are presented in Ref. [30]. The objective of this paper is to present the extension of this theory to shells of relatively small curvature. In this case, the rays are curved and obtained using an asymptotic development with a small parameter h/R (h is the thickness and R the radius of curvature). This extension was introduced into the program COmplex RAYs for Medium Frequencies (CORAY MF) developed by Rouch at the LMT Cachan and the results were compared to NASTRAN's.

2. The reference problem

In order to simplify the presentation, the problem will be formulated for an assembly of two substructures, but this can be easily generalized to the case of n substructures. Two isotropic

homogeneous shells with Σ and Σ' as their reference surfaces are considered. $\partial\Sigma$ and $\partial\Sigma'$ denote the boundaries of Σ and Σ' respectively. It is required to study the harmonic vibration of these two structures at a fixed frequency ω. All quantities can be defined in the complex domain: an amplitude $\mathbf{Q}(\mathbf{X})$ corresponds to $\mathbf{Q}(\mathbf{X})e^{i\omega t}$. For each shell, the displacement $\mathbf{u} = (\mathbf{v}, w)$ (tangential displacement $\mathbf{v}$, normal displacement w), the moment and the resultant (associated with operators $\mathbf{M}$ and $\mathbf{N}$ respectively) are taken into account. The structures are assumed to be slightly curved. The action of the environment on Σ is represented in Fig. 1 and consists of a displacement field $\mathbf{u}_d$ on $\partial_{\mathbf{u}_d}\Sigma$, a force density $\mathbf{F}_d$ on $\partial_{\mathbf{F}_d}\Sigma$ and a surface load $\mathbf{f_d}$ on Σ. Similar quantities are defined on Σ'.

The shell theory used here is Koiter's linear theory (see Refs. [31–33]). The displacement class is restricted to $\mathbf{U} = \mathbf{v} + w\mathbf{e_3} + z\beta$ (Kirchhoff's kinematic assumption) with $\beta = \boldsymbol{\nabla}(w) - \mathbf{B}\,\mathbf{v}$, where $\mathbf{B}$ is the curvature tensor. The transverse deformation energy is neglected.

Define for the structure Σ the field $\Sigma_{ad} = \{(\mathbf{v}, w, \mathbf{N}, \mathbf{M})\}$ such that

$$(\mathbf{v}, w) \in \mathbf{U} \quad \text{finite} - \text{energy displacement set,}$$
$$(\mathbf{N}, \mathbf{M}) \in \mathbf{S} \quad \text{finite} - \text{energy generalized stress set,}$$
$$\mathbf{div}\,\mathbf{N} - \mathbf{B}(\mathbf{div}\,\mathbf{M}) + \mathbf{f_d} = -\omega^2\rho(1 - i\theta)\mathbf{v} \quad \text{on } \Sigma,$$
$$div(\mathbf{div}\,\mathbf{M}) + Tr(\mathbf{N}\,\mathbf{B}) = -\omega^2\rho(1 - i\theta)w \quad \text{on } \Sigma,$$
$$\mathbf{M} = \frac{h^3}{12}(1 + i\eta)K_{CP}\,\mathbf{X}(\mathbf{u}) \quad \text{on } \Sigma,$$
$$\mathbf{N} = h(1 + i\eta)K_{CP}\,\gamma(\mathbf{u}) \quad \text{on } \Sigma,$$
$$\mathbf{X}(\mathbf{u}) = \varepsilon(\beta) - [\mathbf{B}\,\varepsilon(\mathbf{v} + w\mathbf{e_3})]_{sym},$$
$$\gamma(\mathbf{u}) = \varepsilon(\mathbf{v} + w\mathbf{e_3}), \tag{1}$$

where K_{CP} is Hooke's plane stress operator, ρ the density, θ and η the (frequency dependent) damping coefficients and h the thickness of the shell. Σ'_{ad} is defined in the same way. The subspaces Σ_{ad} and Σ'_{ad} associated with the homogenized conditions ($\mathbf{f_d} = \mathbf{f'_d} = \mathbf{0}$) are denoted Σ_{ad0} and Σ'_{ad0}. Thus, the problem to be solved can be expressed as: find $(\mathbf{v}, w, \mathbf{N}, \mathbf{M}) \in \Sigma_{ad}$ and $(\mathbf{v}', w', \mathbf{N}', \mathbf{M}') \in \Sigma'_{ad}$
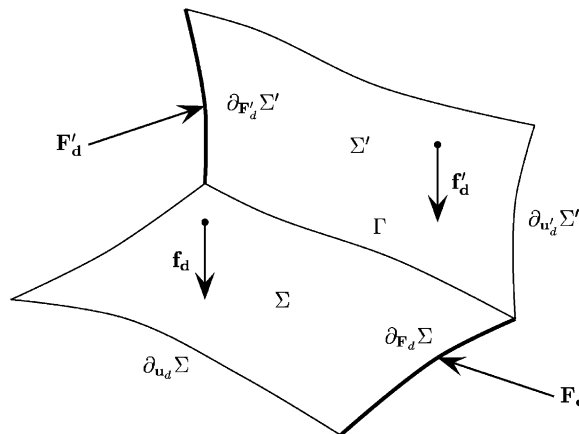

Fig. 1. Problem definition.

which verify the boundary conditions:

$$\mathbf{v} = \mathbf{v}_d \quad \text{on } \partial_{\mathbf{v}_d}\Sigma, \qquad\qquad \mathbf{v}' = \mathbf{v}'_d \quad \text{on } \partial_{\mathbf{v}'_d}\Sigma',$$

$$w = w_d \quad \text{on } \partial_{w_d}\Sigma, \qquad\qquad w' = w'_d \quad \text{on } \partial_{w'_d}\Sigma',$$

$$w_{,n} = w_{nd} \quad \text{on } \partial_{w_{nd}}\Sigma, \qquad\qquad w'_{,n} = w'_{nd} \quad \text{on } \partial_{w'_{nd}}\Sigma',$$

$$\mathbf{N\,n} - \mathbf{B\,M\,n} = \mathbf{N}_d \quad \text{on } \partial_{\mathbf{N}_d}\Sigma, \qquad \mathbf{N'n'} - \mathbf{B\,M'n'} = \mathbf{N}'_d \quad \text{on } \partial_{\mathbf{N}'_d}\Sigma',$$

$$(\mathbf{div\,M})^\top \mathbf{n} + (\mathbf{n}^\top \mathbf{M\,t})_{,t} = K_d \qquad (\mathbf{div\,M'})^\top \mathbf{n'} + (\mathbf{n'}^\top \mathbf{M'\,t'})_{,t} = K'_d$$

$$\qquad \text{on } \partial_{K_d}\Sigma, \qquad\qquad\qquad \text{on } \partial_{K'_d}\Sigma',$$

$$\mathbf{n}^\top \mathbf{M\,n} = M_d \quad \text{on } \partial_{M_d}\Sigma, \qquad \mathbf{n'}^\top \mathbf{M'n'} = M'_d \quad \text{on } \partial_{M'_d}\Sigma',$$

$$[[\mathbf{n}^\top \mathbf{M\,t}]] = 0 \quad \text{on the corner of } \partial\Sigma, \quad [[\mathbf{n'}^\top \mathbf{M't'}]] = 0 \quad \text{on the corner of } \partial\Sigma',$$

$$\mathbf{v} = \mathbf{v}' \quad \text{on } \Gamma,$$

$$w = w' \quad \text{on } \Gamma,$$

$$w'_n = w'_{,n} \quad \text{on } \Gamma,$$

$$\mathbf{N\,n} - \mathbf{B\,M\,n} = \mathbf{N'n'} - \mathbf{B'\,M'n'} \quad \text{on } \Gamma,$$

$$(\mathbf{div\,M})^\top \mathbf{n} + (\mathbf{n}^\top \mathbf{M\,t})_{,t} = (\mathbf{div\,M'})^\top \mathbf{n'} + (\mathbf{n'}^\top \mathbf{M'\,t'})_{,t} \quad \text{on } \Gamma,$$

$$\mathbf{n}^\top \mathbf{M\,n} = \mathbf{n'}^\top \mathbf{M'n'} \quad \text{on } \Gamma. \tag{2}$$

3. The variational formulation associated with the VTCR

The VTCR is a global formulation of the boundary conditions 2 in displacements as well as in forces. The theory uses a priori independent approximations within the substructures: find $(\mathbf{v}, w, \mathbf{N}, \mathbf{M}) \in \Sigma_{ad}$ and $(\mathbf{v}', w', \mathbf{N}', \mathbf{M}') \in \Sigma'_{ad}$ such that

$$\text{Re}\Bigg\{ -\mathrm{i}\omega \Bigg[\int_{\partial_{\mathbf{v}_d}\Sigma} \delta\mathbf{N}_n^\top \cdot (\mathbf{v} - \mathbf{v}_d)^* \, \mathrm{d}L + \int_{\partial_{\mathbf{N}_d}\Sigma} (\mathbf{N}_n - \mathbf{N}_d)^\top \cdot \delta\mathbf{v}^* \, \mathrm{d}L$$

$$- \int_{\partial_{w_{nd}}\Sigma} \delta M_n \cdot (w_{,n} - w_{nd})^* \, \mathrm{d}L - \int_{\partial_{M_d}\Sigma} (M_n - M_d) \cdot \delta w_{,n}^* \, \mathrm{d}L$$

$$+ \int_{\partial_{w_d}\Sigma} \delta K_n (w - w_d)^* \, \mathrm{d}L + \int_{\partial_{K_d}\Sigma} (K_n - K_d) \delta w^* \, \mathrm{d}L$$

$$+ \int_{\partial_{\mathbf{v}'_d}\Sigma} \delta\mathbf{N}_n'^\top \cdot (\mathbf{v}' - \mathbf{v}'_d)^* \, \mathrm{d}L + \int_{\partial_{\mathbf{N}'_d}\Sigma} (\mathbf{N}'_n - \mathbf{N}'_d)^\top \cdot \delta\mathbf{v}'^* \, \mathrm{d}L$$

$$- \int_{\partial_{w'_{nd}}\Sigma} \delta M'_n \cdot (w'_{,n} - w'_{nd})^* \, \mathrm{d}L - \int_{\partial_{M'_d}\Sigma} (M'_n - M'_d) \cdot \delta w'^*_{,n} \, \mathrm{d}L$$

$$+ \int_{\partial_{w'_d}\Sigma} \delta K'_n (w' - w'_d)^* \, \mathrm{d}L + \int_{\partial_{K'_d}\Sigma} (K'_n - K'_d) \delta w'^* \, \mathrm{d}L$$

$$+ \sum_{\partial\Sigma \text{ corner}} [[\mathbf{n}^\top \mathbf{M}\, \mathbf{t}]]\delta w^* + \sum_{\partial\Sigma' \text{ corner}} [[\mathbf{n}'^\top \mathbf{M}'\mathbf{t}']]\delta w'^*$$

$$+ \int_\Gamma \tfrac{1}{2}[(\delta\mathbf{N}_n - \delta\mathbf{N}'_n)^\top(\mathbf{v} - \mathbf{v}')^* - (\delta M_n + \delta M'_n)(w_{,n} + w'_{,n})^*$$

$$+ (\delta K_n - \delta K'_n)(w - w')^*]\,\mathrm{d}L + \int_\Gamma \tfrac{1}{2}[(\mathbf{N}_n + \mathbf{N}'_n)^\top(\delta\mathbf{v} + \delta\mathbf{v}')^*$$

$$- (M_n - M'_n)(\delta w_{,n} - \delta w'_{,n})^* + (K_n + K'_n)(\delta w + \delta w')^*]\,\mathrm{d}L$$

$$= 0,$$

$$\forall\,(\delta\mathbf{v}, \delta w, \delta\mathbf{N}, \delta\mathbf{M}) \in \Sigma_{ad0} \quad \text{and} \quad (\delta\mathbf{v}', \delta w', \delta\mathbf{N}', \delta\mathbf{M}') \in \Sigma'_{ado},$$

where Re[A] designates the real part of A and A^* the conjugate of A. It can easily be proved (see Ref. [29]) that the variational formulation is equivalent to the reference problem if:

- the reference problem has a solution,
- Hooke's tensor is positive definite,
- the damping factors are greater than zero.

It is possible to reformulate the problem as: find $s = (\mathbf{v}, w, \mathbf{N}, \mathbf{M}) \in \Sigma_{ad}$ and $s' = (\mathbf{v}', w', \mathbf{N}', \mathbf{M}') \in \Sigma'_{ad}$ such that

$$\delta(E_D(\mathbf{u}) + E'_D(\mathbf{u}')) + \langle(s, s'), \delta(s, s')\rangle = (L_D, \delta(s, s')),$$

$$\forall \delta s \in \Sigma_{ad0} \quad \forall \delta s' \in \Sigma'_{ad0}.$$

where E_D is the dissipation power, L_D a linear form and $\langle.,.\rangle$ a bilinear form defined on the substructure boundaries which verifies $\langle u, v\rangle = -\langle v^*, u^*\rangle$.

4. Approximation of the VTCR

4.1. Principle

In order to develop approximations for the VTCR, the subspaces can be defined as Σ^h_{ad} and Σ'^h_{ad}. An approximate formulation can be written as: find $s^h \in \Sigma^h_{ad}$ and $s'^h \in \Sigma'^h_{ad}$ such that

$$\delta(E_D(\mathbf{u}^h) + E'_D(\mathbf{u}'^h)) + \langle(s^h, s'^h), \delta(s^h, s'^h)\rangle = (L_D, \delta(s^h, s'^h))$$

$$\forall(\delta s^h, \delta s'^h) \in \Sigma^h_{ad0} \times \Sigma'^h_{ad0}.$$

The VTCR uses two-scale approximations with a strong mechanical meaning by considering three different types of zones: the interior zone, the edge zones, and the corner zones. For example, in the vicinity of a point $\mathbf{X}$ in the interior zone, the solution is assumed to be well-described locally as the superposition of an infinite number of local vibration modes which can be written as

$$\mathbf{U}(\mathbf{X}, \mathbf{Y}, \mathbf{P}) = \mathbf{W}(\mathbf{X}, \mathbf{Y}, \mathbf{P})e^{\mathrm{i}\omega\mathbf{P}\cdot\mathbf{Y}},$$

where both $\mathbf{X}$ and $\mathbf{Y}$ represent the position vector, but $\mathbf{X}$ is associated with a slow variation and $\mathbf{Y}$ with a fast variation. $\mathbf{P}$ is a vector which characterizes the local vibration mode. The modes are

defined explicitly in terms of the fast variable and, therefore, the unknowns consist only of large-wavelength quantities.

4.2. Zeroth order complex rays

Given a homogeneous substructure, consider, for simplicity's sake, the case where there is no force density ($\mathbf{f_d} = \mathbf{0}$). The numerical examples presented in this paper use zeroth order complex rays, i.e., $\mathbf{W}(\mathbf{X}, \mathbf{Y}, \mathbf{P}) = \mathbf{W}(\mathbf{P})$. For the plate, neglecting the membrane behaviour, it can be shown (see Ref. [30]) that a zeroth order complex ray is admissible only if:

$$(\mathbf{P}^\top \mathbf{P})^2 = \left(\frac{1 - i\theta}{1 + i\eta}\right)\frac{12\rho(1 - v^2)}{Eh^2\omega^2}. \tag{3}$$

For shells, an explicit form of the vector $\mathbf{P}$ cannot be found. However, (1) can be written as:

$$\mathbf{div}(K_{CP}\gamma(\mathbf{u}) - \frac{h^2}{12}\mathbf{B}\,\mathbf{div}(K_{CP}\mathbf{X}(\mathbf{u}))) = -\frac{\omega^2\rho}{h}\frac{(1 - i\theta)}{(1 + i\eta)}\mathbf{v}, \tag{4}$$

$$\frac{h^2}{12}\,div(\mathbf{div}(K_{CP}\mathbf{X}(\mathbf{u}))) + Tr(K_{CP}\gamma(\mathbf{u})\mathbf{B}) = -\frac{\omega^2\rho}{h}\frac{(1 - i\theta)}{(1 + i\eta)}w, \tag{5}$$

$$\mathbf{X}(\mathbf{u}) = \varepsilon(\beta) - [\mathbf{B}\,\varepsilon(\mathbf{v} + w\mathbf{e_3})]_{sym},$$

$$\gamma(\mathbf{u}) = \varepsilon(\mathbf{v} + w\mathbf{e_3}),$$

$$\beta = -\mathbf{\nabla}(w) - \mathbf{B}\mathbf{v}.$$

A linear equation must be solved with a small parameter multiplying the highest derivative term. The solution to this equation can be found using an asymptotic analysis (see Ref. [34]). The large parameter is $\lambda = (12R^2/h^2)^{1/4}$, where R represents the smallest radius of curvature of the whole structure. An asymptotic expansion for the solution can be obtained by assuming the form:

$$\begin{pmatrix} \mathbf{v} \\ w \end{pmatrix} = \left(\begin{pmatrix} \mathbf{v}_0 \\ w_0 \end{pmatrix} + \frac{1}{\lambda}\begin{pmatrix} \mathbf{v}_1 \\ w_1 \end{pmatrix} + \frac{1}{\lambda^2}\begin{pmatrix} \mathbf{v}_2 \\ w_2 \end{pmatrix} + \dots \right)e^{\lambda f}, \tag{6}$$

where f is a scalar function. The method consists of substituting the expansion (6) into Eqs. (4) and (5) and grouping the terms with the same power of λ. Eq. (4) associated with the parameter λ^2 yields

$$K_{CP}([\mathbf{v}_0\mathbf{\nabla}f^\top]_{sym})\mathbf{\nabla}f = \mathbf{0}. \tag{7}$$

The solution to Eq. (7) is

$$\mathbf{v}_0 = \mathbf{0}. \tag{8}$$

Eq. (4) associated with the parameter λ, after taking Eq. (8) into account, yields

$$K_{CP}([\mathbf{v}_1\mathbf{\nabla}f^\top]_{sym})\mathbf{\nabla}f - K_{CP}(\mathbf{B}w_0)\mathbf{\nabla}f = \mathbf{0} \tag{9}$$

which can be solved easily. Indeed, if

$$\mathbf{v}_1 = \alpha\mathbf{\nabla}f + \beta\mathbf{R}\,\mathbf{\nabla}f, \tag{10}$$

where

$$\mathbf{R} = \begin{pmatrix} 0 & -1 \\ 1 & 0 \end{pmatrix}^{1},$$

the solution is

$$\alpha = w_0 \frac{\nabla f^\top \tilde{K}_{CP}(\mathbf{B})\nabla f}{(\nabla f^\top \nabla f)^2}, \tag{11}$$

$$\beta = \frac{2}{1-v} \frac{\nabla f^\top \tilde{K}_{CP}(\mathbf{B})\mathbf{R}\,\nabla f}{(\nabla f^\top \nabla f)^2}, \tag{12}$$

where $\tilde{K}_{CP} = (1 - v^2)K_{CP}$. Finally, Eq. (5) associated with the parameter λ^0, after taking into account Eqs. (10)–(12), yields;

$$-E(\nabla f^\top \nabla f)^2 w_0 + \frac{1}{R^2} Tr(\mathbf{N}(\mathbf{v}_1, w_0)\mathbf{B}) = -\frac{\omega^2 \rho(1-v^2)}{hR^2}\frac{(1-i\theta)}{(1+i\eta)} w_0, \tag{13}$$

where $\mathbf{N}(\mathbf{v}_1, w_0) = \tilde{K}_{CP}[\mathbf{v}_1 \nabla f^\top]_{sym} - \tilde{K}_{CP}(\mathbf{B}w_0)$.

Eq. (9) shows that $\mathbf{N}(\mathbf{v}_1, w_0)\nabla f = \mathbf{0}$. Therefore,

$$\mathbf{N}(\mathbf{v}_1, w_0) = Tr(\mathbf{N}(\mathbf{v}_1, w_0))\frac{(\mathbf{R}\nabla f)(\mathbf{R}\nabla f)^\top}{(\mathbf{R}\nabla f)^\top(\mathbf{R}\nabla f)} = \frac{(\mathbf{R}\nabla f)(\mathbf{R}\nabla f)^\top}{\nabla f^\top \nabla f} \tag{14}$$

and, therefore

$$Tr(\mathbf{N}(\mathbf{v}_1, w_0)\mathbf{B}) = -Tr(\mathbf{N}(\mathbf{v}_1, w_0))\frac{\nabla f^\top \mathbf{R}\,\mathbf{B}\,\mathbf{R}\,\nabla f}{\nabla f^\top \nabla f}. \tag{15}$$

Using Eq. (10) and knowing that

$$Tr(\mathbf{N}(\mathbf{v}_1, w_0)) = \frac{(\nabla f)^\top \mathbf{N}(\mathbf{v}_1, w_0)(\nabla f)}{\nabla f^\top \nabla f} - \frac{(\nabla f)^\top \mathbf{R}\,\mathbf{N}\,\mathbf{R}(\mathbf{v}_1, w_0)(\nabla f)}{\nabla f^\top \nabla f}$$

it can easily be shown that

$$Tr(\mathbf{N}(\mathbf{v}_1, w_0)) = (1 - v^2)w_0 \frac{\nabla f^\top \mathbf{R}\,\mathbf{B}\,\mathbf{R}\,\nabla f}{\nabla f^\top \nabla f}. \tag{16}$$

Substituting Eqs. (15) and (16) into Eq. (13) and eliminating w_0, gives the dispersion equation:

$$(\nabla f^\top \nabla f)^4 = \frac{\omega^2 \rho(1-v^2)}{hR^2 E}\frac{(1-i\theta)}{(1+i\eta)}(\nabla f^\top \nabla f)^2 - \frac{(1-v^2)}{R^2}(\nabla^\top \mathbf{R}\,\mathbf{B}\,\mathbf{R}\,\nabla f)^2. \tag{17}$$

---

[1] $\mathbf{R}$ is a rotation matrix, $\mathbf{R}^\top = -\mathbf{R}$. ∇f and $\mathbf{R}\,\nabla f$ are orthogonal vectors and form a basis.

In this case, $\lambda \nabla f = \omega \mathbf{P}$. Eqs. (8), (10)–(12) and (17) become

$$\mathbf{v} = \left(\frac{1}{\omega} \frac{\mathbf{P}^\top \tilde{K}_{CP}(\mathbf{B})\mathbf{P}}{(\mathbf{P}^\top \mathbf{P})^2} \mathbf{P} - \frac{2}{(1-v)\omega} \frac{\mathbf{P}^\top \tilde{K}_{CP}(\mathbf{B})\mathbf{R}\,\mathbf{P}}{(\mathbf{P}^\top \mathbf{P})^2} \mathbf{RP} \right) w_0, \tag{18}$$

$$(\mathbf{P}^\top \mathbf{P})^4 = \left(\frac{1-i\theta}{1+i\eta} \right) \frac{12\rho(1-v^2)}{Eh^2\omega^2} (\mathbf{P}^\top \mathbf{P})^2 - \frac{12(1-v^2)}{\omega^4 h^2} (\mathbf{P}^\top \mathbf{RBRP})^2. \tag{19}$$

A particular complex ray is admissible only if $\mathbf{P}$ verifies Eq. (19).

Remark 1. This equation is the same as that in Ref. [35].

Remark 2. If the radius of curvature tends towards infinity (i.e., if the shell tends towards a plate), $\mathbf{B}$ tends towards 0 and this reverts to Eq. (3).

Remark 3. Eq. (18) shows that the tangential displacement is completely determined once the normal displacement w_0 is known. Therefore, only w_0 needs to be sought.

Remark 4. It can be seen that the term w alone is present in the development of $\mathbf{M}$. This explains why Eqs. (18) and (19) are valid with other shell theories, provided that $\gamma(\mathbf{u}) = \varepsilon(\mathbf{v} + w\mathbf{e_3})$. This is the case for the theories of Love, Timoshenko, Reissner, Naghdi, Berry, Dowell and Mushtari (see Ref. [33]).

Remark 5. The zeroth order complex ray can be considered as the first term of an asymptotic development where the small parameter is the factor $1/\omega$. This is a well-known concept in geometric optics [36,37].

4.3. Zeroth order complex rays for a cylinder

In order to illustrate Eq. (19), consider a cylindrical shell. The co-ordinates to be used are z and θ (the longitudinal and angular variables respectively). R is the radius of curvature. A zeroth order complex ray is written as $\mathbf{W}(\mathbf{P})e^{i\omega \mathbf{P}^\top \mathbf{X}} = \mathbf{W}(\mathbf{P})e^{i\omega(P_\theta R\theta + P_z z)}$. The curvature tensor is

$$\mathbf{B} = \begin{pmatrix} -\frac{1}{R} & 0 \\ 0 & 0 \end{pmatrix}.$$

4.3.1. Complex rays for the interior zone
The rays for the interior zone are sought such that they verify Eq. (19) and correspond to a propagative solution. They can be written as

$$\begin{pmatrix} P_\theta \\ P_z \end{pmatrix} = P(\varphi) \begin{pmatrix} \cos \varphi \\ \sin \varphi \end{pmatrix},$$

with $P(\varphi)$ verifying

$$P^4(\varphi) = P_0^4 \left(\frac{1 - i\theta}{1 + i\eta} \right) - P_C^4 \sin^4 \varphi,$$

$$P_0^4 = \frac{12\rho(1 - v^2)}{E\omega^2 h^2},$$

$$P_C^4 = \frac{12(1 - v^2)}{\omega^4 h^2 R^2}. \tag{20}$$

Whenever possible, take $\text{Re}(P(\varphi)) \gg \text{Im}(P(\varphi))$ in order to enforce propagative behaviour. Fig. 2 shows such rays for $\varphi = 0°$, $\varphi = 45°$ and $\varphi = 90°$.

4.3.2. Complex rays for the edge zones

The rays for the edge zones are sought such that they verify Eq. (19) and vanish far away from the edge. Furthermore, the edge rays must not oscillate faster than the interior rays. One option is to take $\text{Re}(\mathbf{P}^\top(\varphi))\mathbf{t} = \text{Re}(\mathbf{P}_{int}^\top(\varphi))\mathbf{t}$, $\text{Im}(\mathbf{P}^\top(\varphi))\mathbf{t} = 0$ and $\text{Im}(\mathbf{P}^\top(\varphi))\mathbf{n} \gg \text{Re}(\mathbf{P}^\top(\varphi))\mathbf{n}$ (where $\mathbf{P}_{int}(\varphi)$ is the ray for the interior zone in the direction φ and $\mathbf{t}$ and $\mathbf{n}$ are respectively the tangent and normal vectors with respect to the edge). Fig. 3 shows such rays.

4.3.3. Complex rays for the corner zones

The rays for the corner zones are sought such that they verify Eq. (19) and vanish far away from the corner. They can be written in the same way as the rays for the edge zones, but in a local basis associated with the corner (the bisector and a perpendicular vector). Fig. 4 shows such rays.
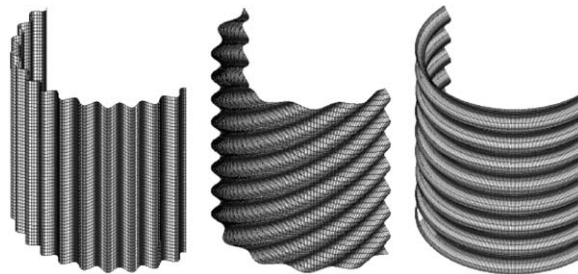

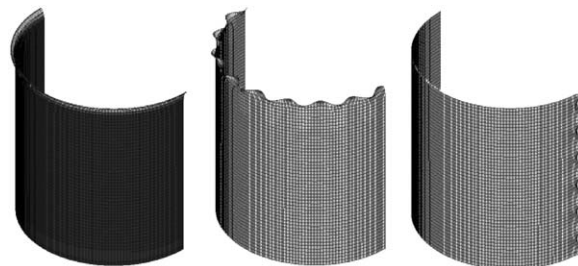Fig. 2. Complex rays for the interior zone of the cylinder.

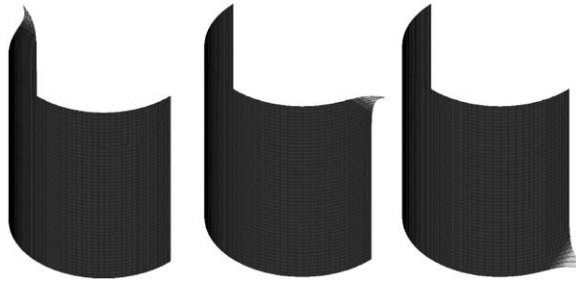Fig. 3. Complex rays for the edge zones of the cylinder.

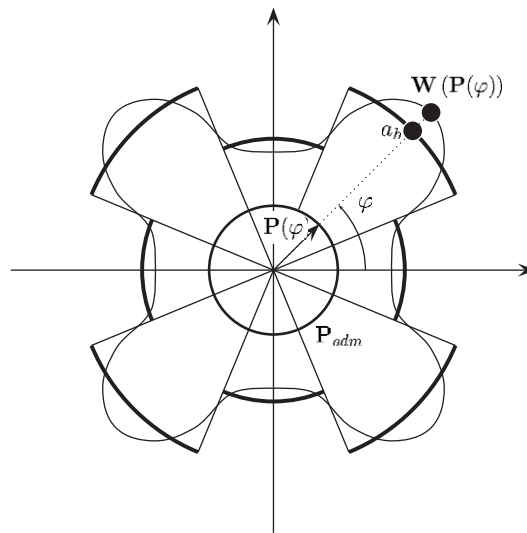Fig. 4. Complex rays for the corner zones of the cylinder.

Fig. 5. Discretized amplitudes.

4.4. The discretized problem

Assuming that the solution can be properly described by a linear combination of zeroth order complex rays, it can be written as

$$\mathbf{W}(\mathbf{X}, \mathbf{Y}) = \int_{\mathbf{P} \in \mathbf{P}_{ad}} \mathbf{W}(\mathbf{P}) \, e^{i\omega \mathbf{P}^\top \mathbf{Y}} \, ds_p,$$

where $\mathbf{P}_{ad}$ is the curve which follows $\mathbf{P}$ verifying Eq. (19). $\mathbf{P}_{ad}$ can be discretized using finite elements. $\mathbf{W}(\mathbf{P})$ is assumed to be constant within each element: $\mathbf{W}(\mathbf{P}) = H^h(\mathbf{P}) \, a^h$ (see Fig. 5). a^h is the unknown generalized amplitude. Thus, the VTCR uses two functions defined on different scales:

- the fast scale (complex exponential), which is calculated explicitly,
- the slow scale, which is discretized.

4.5. Generalized amplitude

In order to solve the medium-frequency problem, it is necessary to extract generalized quantities from the above solution. The spatial distribution of the solution has no physical meaning from the mechanical point of view. The effective displacement U_{eff} on a domain D, which corresponds to the average displacement on the domain D is used:

$$U_{eff} = \frac{1}{D} \int_D |w(\alpha, \beta)| \, \mathrm{d}D.$$

5. Application

5.1. Preliminary remarks: convergence of the finite element and VTCR methods

It is widely accepted that the sizes of the elements in a finite-element-based calculation should be set in relation to the wavelength. In many cases, engineering practice determines the number of elements per wavelength for constant, linear or bilinear elements. This number varies between six and ten. Undoubtedly, this number is closely related to a certain desired accuracy. Often, the acceptable magnitude of the error depends on the user and on the technical requirements of the problem (see Ref. [38]). In Ref. [13], the study of the finite element analysis confirmed the common rule of engineering practice mentioned above. This rule, often formulated with six elements per wavelength, is written as $kh < 1$ (k wave number, h element size), which corresponds to about 6.3 elements per wavelength. This is a reliable rule for finite element approximations at low wave numbers, but for higher wave numbers it must be modified. In the latter case, studies based on the dispersion and pollution of the finite element solution [5,7] show that a more reliable rule is to set $k^3 h^2$ equal to a constant.

The convergence rate of the finite element method was tested for a simple case. The half-cylinder defined in Fig. 6 was considered, subjected to a distributed load. The structure's material
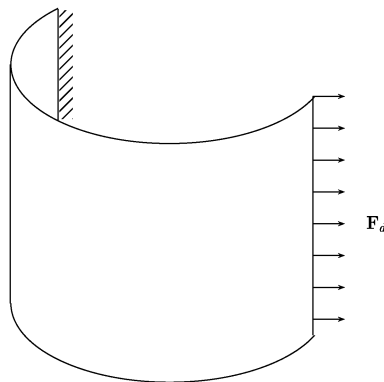

Fig. 6. Geometry model of the half-cylinder: the cylinder is fixed at one end and a force density $\mathbf{F}_d$ is applied at the other end.

has the following characteristics: $E = 75$ GPa, $\eta = 0.0001$, $\theta = 0$, $v = 0.3$, $\rho = 2750$ kg/m^3, $\omega = 1800$ Hz, $F_d = 1$ N/m.

The finite element solutions were calculated with the NASTRAN program. Different numbers of elements per wavelength were tested $(1, 2, 3, 4, 5, 8, 10,$ and $20)$. All the finite element meshes consisted of identical quadrilateral shell elements. Since comparison of the solutions with respect to effective quantities was required, the effective displacement over the whole structure was calculated for each mesh (which corresponds to the average displacement and, in medium-frequency analysis, has more physical meaning than the displacement of a point). The results are presented in Fig. 7.

It can reasonably be assumed that the solution with 20 elements per wavelength is very accurate. Therefore, the corresponding effective displacement was considered as the reference. It can be seen that with $1, 2, 3, 4$ and 5 elements per wavelength the result is quite poor. With 8 and 10 elements per wavelength, the magnitude of the effective displacement is good. Such mesh sizes would be acceptable for the calculation of effective quantities. Nevertheless, having looked at the local displacements, 10 elements per wavelength were chosen. In the following sections, all finite element solutions obtained with NASTRAN were calculated using this rule.

Concerning the convergence rate of the VTCR, the method on the same case (Fig. 6) was tested. Different numbers of interior and edge modes were tested. The corner modes were not taken into account, since these are involved only when a point force is applied at a corner of the structure. Again, the effective displacement of the whole structure was calculated. The results are given in Fig. 8 (only the cases 0 and 1 edge mode per edge are shown; more edge modes per edge give even better results).

Although the structure being considered is very simple, some rules can be derived. The edge modes are essential. If they are not taken into account, convergence cannot be achieved, even by increasing the number of interior modes. The influence of the edge modes is primarily on the local
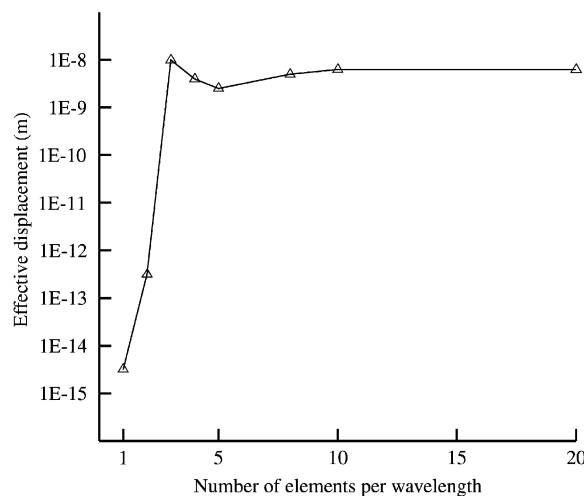

Fig. 7. Effective displacement of the whole structure of the half-cylinder (Fig. 6) for different numbers of finite elements per wavelength. 20 elements per wavelength is a sufficiently large number to be considered as the reference.
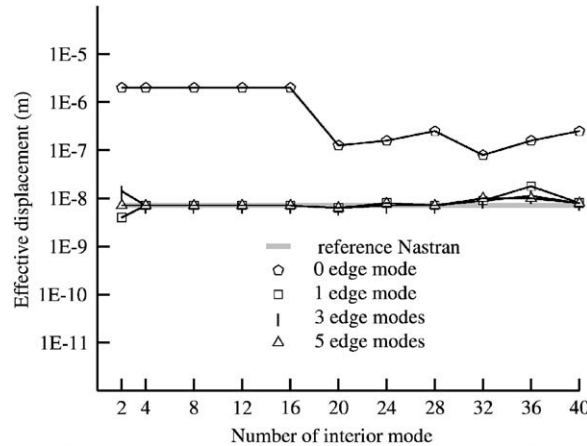
Fig. 8. Effective displacement of the whole structure of the half-cylinder (Fig. 6) for different numbers of modes using the VTCR. The effective displacement found using NASTRAN is shown in grey.

displacements, especially along the edges. From here on about 20 interior modes, and 5 edge modes per edge will often be used.

5.2. The half-cylinder example

Consider the shell structure described in Fig. 6. The mechanical properties are: $E = 75$ GPa, $\eta = 0.0001$, $\theta = 0$, $v = 0.3$, $\rho = 2750$ kg/m^3, $\omega = 1800$ Hz, $F_d = 1$ N/m. The solution obtained by NASTRAN was used as the reference solution. The mesh seed used in NASTRAN was set to create 10 elements per wavelength. The solution was obtained with 225,000 DOFs. The VTCR solution used 80 DOFs (20 interior modes, 5 edge modes per edge and 0 corner mode). It can be seen in Fig. 9 that the results given by the VTCR are satisfactory: the two solutions in terms of displacements (distribution of the peaks as well as magnitudes) are similar.

In order to compare the different solutions using an effective quantity (which, in medium-frequency analysis, has more physical meaning than the displacement of a point), the effective displacement of the entire structure was calculated. Table 1 shows the comparison in terms of computation time and effective displacement. The computation time is the sum of the times required for calculating and inverting the stiffness matrix.

5.3. Use of substructures

Consider the problem of Fig. 6 again. The mechanical properties are: $E = 75$ GPa, $\eta = 0.0001$, $\theta = 0$, $v = 0.3$, $\rho = 2750$ kg/m^3, $\omega = 1800$ Hz, $F_d = 1$ N/m. Now, the half-cylinder is partitioned into two substructures along the line Γ, as shown in Fig. 10. The solution obtained by the VTCR used 160 DOFs (20 interior modes, five edge modes per edge and zero corner mode for each substructure). The results are satisfactory. On the right-hand side of Fig. 11 (axial separation), a small discontinuity at the interface Γ can be seen. Thanks to the variational formulation, the
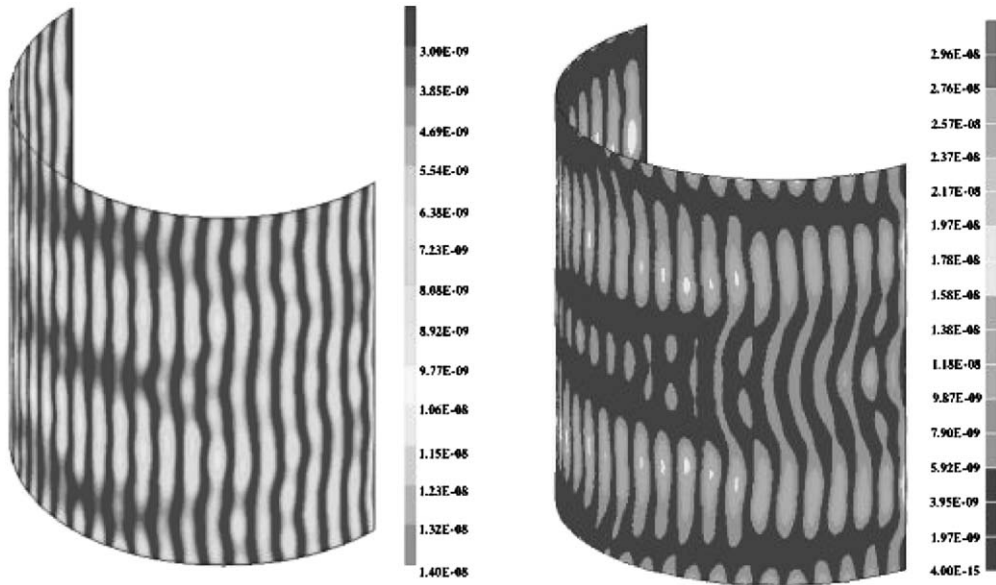
Fig. 9. Results for the half-cylinder problem (Fig. 6): VTCR solution (left) and NASTRAN solution (right). These two solutions are similar in local displacement: the distribution of the peaks is the same and their magnitudes are about 1.0×10^{-8} for the VTCR solution and 1.2×10^{-8} for the NASTRAN solution. The maximum magnitude is found on the edge where the force is applied: 1.4×10^{-8} for the VTCR solution and 2.9×10^{-8} for the NASTRAN solution. The slight difference at the edge is due to the fact that for the VTCR the boundary conditions are verified in an average sense.

Table 1
Results for the half-cylinder problem (Fig. 6): comparison in terms of computation time and effective displacement

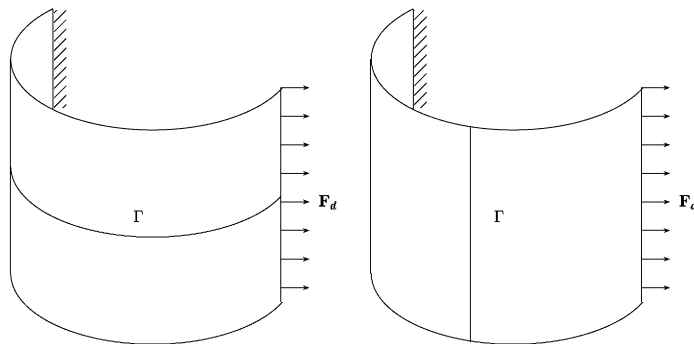|	VTCR	NASTRAN
DOFs	80	225,000
Computation time	3 s	37 s
Effective displacement (m)	6.62×10^{-9} m	6.79×10^{-9} m

Fig. 10. The geometrical model with substructuring: the cylinder is fixed at one end and a force density $\mathbf{F}_d$ is applied at the other end. It is partitioned into two shell substructures along a line Γ: orthoradial on the left and axial on the right.

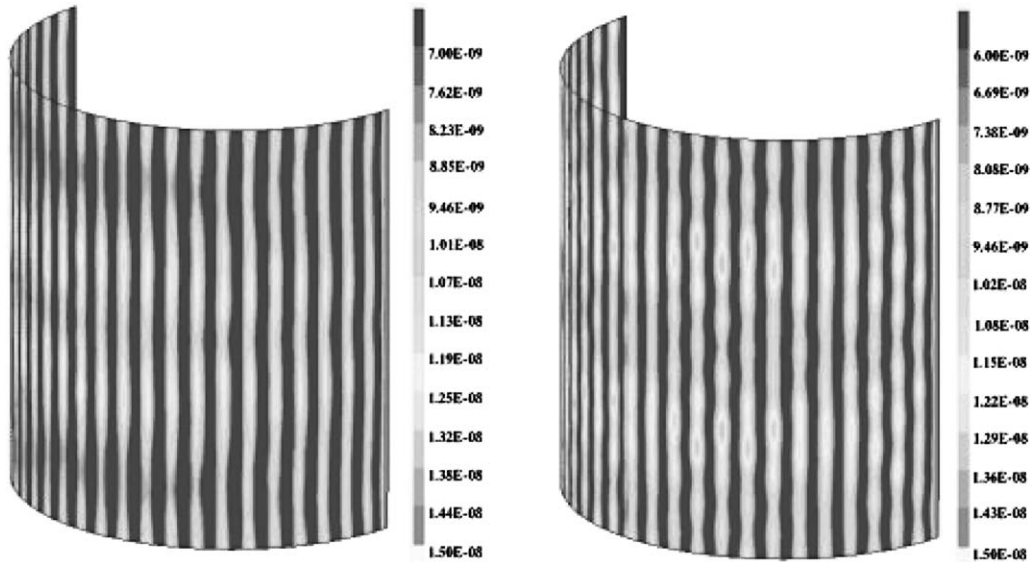| 7.00E-09 | | 6.00E-09 |
7.62E-09		6.69E-09
8.23E-09		7.38E-09
8.85E-09		8.08E-09
9.46E-09		8.77E-09
1.01E-08		9.46E-09
1.07E-08		1.02E-08
1.13E-08		1.08E-08
1.19E-08		1.15E-08
1.25E-08		1.22E-08
1.32E-08		1.29E-08
1.38E-08		1.36E-08
1.44E-08		1.43E-08
1.50E-08		1.50E-08

Fig. 11. Results for the half-cylinder using substructures (Fig. 10): orthoradial partitioning (left) and axial partitioning (right). Both solutions were obtained with the VTCR (which allows substructures) and should be compared with the solution given by NASTRAN (on the right of Fig. 9). The solutions in displacement (distribution and amplitudes) are similar.

transmission conditions at the interface Γ are verified in an average sense. More degrees of freedom would provide better accuracy.

5.4. Curvature effect

One characteristic of the dispersion equation (19) for shells compared to the dispersion equation (3) for plates is that for certain mechanical properties and frequencies there are no modes for the interior zone. Indeed, assuming for the sake of simplicity that there is no damping ($\theta = \eta = 0$), Eq. (20) becomes

$$P^4(\varphi) = P_0^4 - P_C^4 \sin^4 \varphi.$$

If $\omega < (E/\rho R^2)^{1/2}$, then $P_C > P_0$ and for $\varphi = 90°$ $P^4(\varphi) < 0$. In other terms, the longitudinal interior mode necessarily vanishes. The same result can be obtained starting from the shell equation (1). This phenomenon is not due to the asymptotic development; it is a structural property. The additional term in Eq. (19) compared to Eq. (3) is essential. If it is considered that the shell behaves locally like a plate, Eq. (3) must be used and this structural property cannot be observed.

The next example illustrates this case. Consider the shell described in Fig. 12. The mechanical properties are: $E = 75$ GPa, $\eta = 0.0001$, $\theta = 0$, $v = 0.3$, $\rho = 2750$ kg/m^3, $\omega = 500$ Hz, $F_d = 1$ N/m. Then $(E/\rho R^2)^{1/2} = 5222$ rad s$^{-1} = 831$ Hz. Therefore, the conditions for the longitudinal modes to vanish are met. Indeed, it is easy to see that the only possible longitudinal modes are edge modes. Therefore, this example enables the phenomenon just described to be observed.

The solution given by NASTRAN was used as the reference solution. The VTCR solution used 88 DOFs (24 interior modes, five edge modes per edge and zero corner mode). Fig. 13 shows both the VTCR and the NASTRAN solutions. The two solutions are quite similar (there is no vibrational state in the interior domain.)
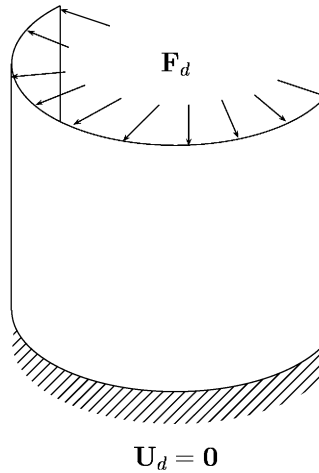

Fig. 12. Shell structure showing the curvature effect: the cylinder is fixed at the bottom and a radial force density $\mathbf{F}_d$ is applied at the top.
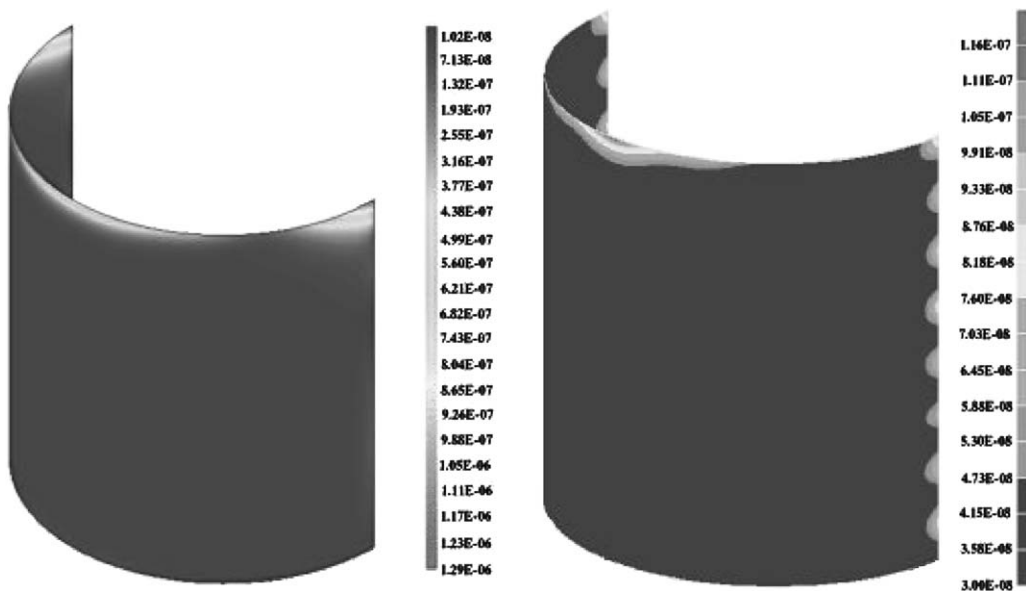

Fig. 13. Result for the half-cylinder with curvature effect (Fig. 12): the VTCR solution (left) and the NASTRAN solution (right) are similar. The NASTRAN solution shows that there is no vibrational state in the interior domain. For the VTCR solution, Eq. (19) shows that the interior modes must vanish and, consequently, that there can be no vibrational state in the interior domain.
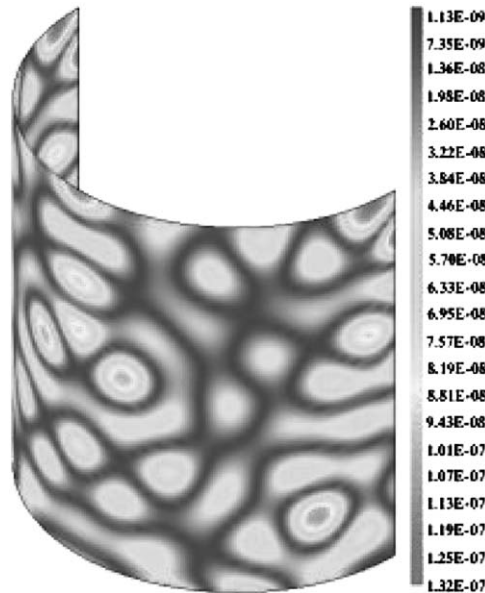
Fig. 14. Result for the half-cylinder with curvature effect (Fig. 12) using Eq. (3) instead of Eq. (19), i.e., without taking into account the curvature effect in shells. A vibrational state in the interior domain is obtained, even though in reality it does not exist (see the NASTRAN solution in Fig. 13). This unacceptable solution shows the importance of the curvature term in Eq. (19).

If Eq. (3) is used (i.e., the shell is seen locally as a plate rather than using Eq. (19), which is suitable for shells), there can be longitudinal modes. The corresponding VTCR solution obtained with the same number of degrees of freedom, shown in Fig. 14, is quite poor. Through this example, the need for the additional term in Eq. (19) because of the curvature can be seen.

5.5. Example of a three-dimensional (3-D) assembly

The geometry defined in Fig. 15 is a 3-D assembly of cylindrical shells and plates. The mechanical properties are: $E = 75$ GPa, $\eta = 0.0001$, $\theta = 0$, $v = 0.3$, $\rho = 2750$ kg/m^3, $\omega = 1000$ Hz, $F_d = 1$ N/m.

The solution obtained by NASTRAN was used as the reference solution. The mesh seed used in NASTRAN was set to create 10 elements per wavelength. The solution was obtained with 1,200,000 DOFs. For the VTCR solution, the structure was divided into three parts (Shell 1, Shell 3 and Plate 2). The calculation used 264 DOFs (24 interior modes, five edge modes per edge and zero corner mode for each substructure). Fig. 16 shows that the results given by the VTCR are good: the two solutions in displacement (distribution and amplitude) are similar.

In order to compare the different solutions with respect to an effective quantity, the effective displacement in each substructure (Shell 1, Shell 3 and Plate 2 (see Fig. 15)) was calculated. Table 2 shows the comparison in terms of computation time and effective displacement. The computation time is the sum of the times required for calculating and inverting the stiffness matrix.
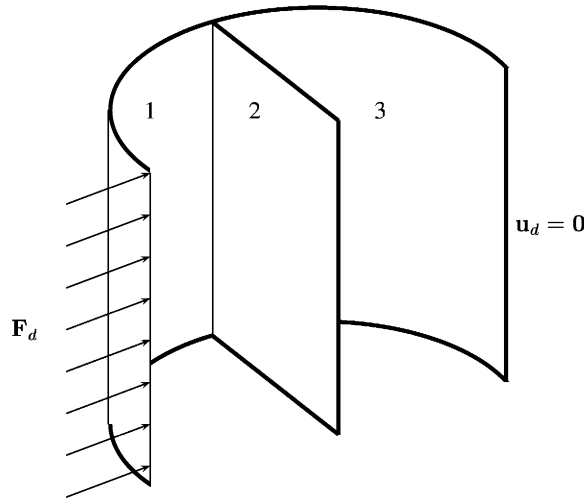
Fig. 15. Geometry of the 3-D assembly. A force density $\mathbf{F}_d$ is applied on one side of Shell 1. All other boundaries are fixed.
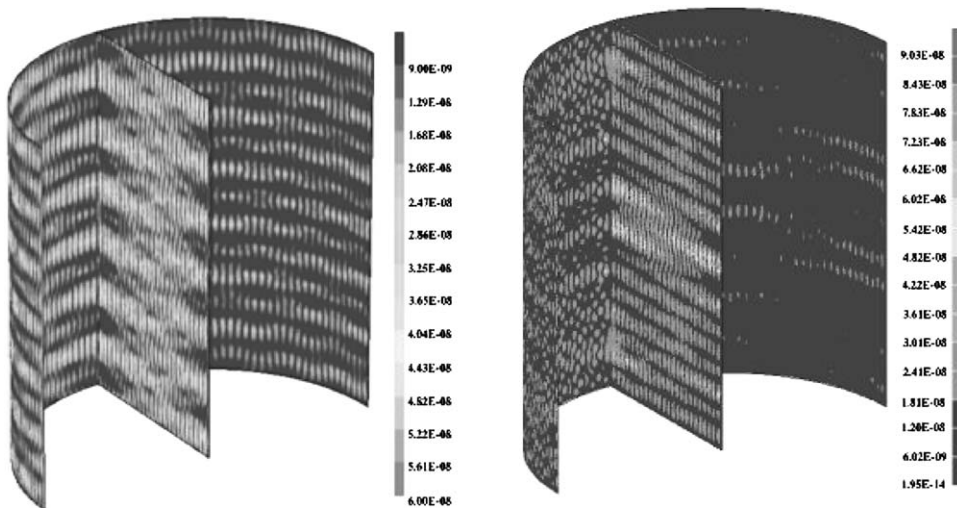

Fig. 16. Results for the 3-D assembly (Fig. 15): the VTCR solution (left) and the NASTRAN solution (right) are similar.

Table 2
Results for the 3-D assembly (Fig. 15): comparison in terms of computation time and effective displacement

	VTCR	NASTRAN
DOFs	264	1,200,000
Computation time	10 s	2 min 32 s
Effective displacement (m)		
Shell 1	1.78×10^{-8}	1.62×10^{-8}
Plate 2	2.57×10^{-8}	2.52×10^{-8}
Shell 3	1.01×10^{-8}	1.09×10^{-8}

It can be seen that the VTCR gives accurate results at a very low cost. The VTCR can calculate any number of homogeneous substructures (plates, shells, etc.) with no particular difficulty.

6. Conclusions

The proposed approach, called the *variational theory of complex rays*, was introduced in order to calculate the vibratory response of weakly damped, slightly curved elastic structures in the medium-frequency range. It is a very general approach with a strong mechanical meaning. Since any industrial structure can reasonably be considered as an assembly of beams (for which the VTCR gives the exact solution), plates and shells, the VTCR seems to be a promising theory for medium-frequency applications.

References

[1] R.H. Lyon, G. Maidanik, Power flow between linearly coupled oscillator, *Journal of the Acoustical Society of America* 34 (5) (1962) 623–639.

[2] E.H. Dowell, Y. Kubota, Asymptotic modal analysis and statistical energy of dynamical systems, *Journal of Applied Mechanics* 52 (1985) 949–957.

[3] B.R. Mace, On the statistical energy analysis hypothesis of coupling power proportionality and some implications of its failure, *Journal of Sound and Vibration* 178 (1) (1994) 95–112.

[4] R.H. Lyon, H. Richard, G. Richard, *Statistical Energy Analysis*, Butterworth-Heinemann, London, 1995.

[5] F. Ihlenburg, I. Babuška, Dispersion analysis and error estimation of Galerkin finite element methods for Helmholtz equation, *International Journal for Numerical Methods in Engineering* 38 (1995) 3745–3774.

[6] P. Bouillard, F. Ihlenburg, Error estimation and adaptativity for the finite element solution in acoustic, *Advance in Adaptative Computational Methods in Mechanics*, Elsevier, Amsterdam, 1998, pp. 477–492.

[7] A. Deraemaeker, I. Babuska, P. Bouillard, Dispersion and pollution of the FEM solution for the Helmholtz equation in one, two and three dimensions, *International Journal for Numerical Methods in Engineering* 46 (1999) 471–499.

[8] L.E. Buvailo, A.V. Ionov, Application of the finite element method to the investigation of the vibroacoustical characteristic of the structures at high frequencies, *Journal of the Soviet Physics Acoustic* 26 (4) (1980) 149–166.

[9] L. Demkowicz, A. Karafiat, J.I. Oden, Solution of elastic scattering problems in linear acoustics using h–p boundary element method, *Computer Methods in Applied Mechanics and Engineering* 101 (1992) 251–282.

[10] I. Harari, J.R. Hugues, Galerkin least squares finite element method for the reduced wave equation with non reflecting boundary condition in unbounded domains, *Computer Methods in Applied Mechanics and Engineering* 98 (1992) 411–454.

[11] I. Babŭska, F. Ihlenburg, E. Paik, S. Sauter, A generalized finite element method for solving the Helmholtz equation in the two dimensions with minimal pollution, *Computer Methods in Applied Mechanics and Engineering* 128 (1995) 325–359.

[12] I. Harari, K. Grosh, J.R. Hugues, M. Malkostra, M. Pinsky, J.R. Steward, L. Thomson, Recent developments in finite element methods for structural acoustic, *Archives of Computational Methods in Engineering* 3 (1996) 131–311.

[13] P.E. Barbone, J.M. Montgommery, O. Michael, I. Harari, Scattering by a hybrid asymptotic/finite element method, *Computer Methods in Applied Mechanics and Engineering* 164 (1998) 141–156.

[14] K. Grosh, P.M. Pinsky, Galerkin generalized least square finite element methods for time harmonic structural acoustic, *Computer Methods in Applied Mechanics and Engineering* 154 (1998) 299–318.

[15] K. Wu, J.H. Ginsberg, Mid frequency range acoustic radiation from slender elastic bodies using the surface variational principle, *Journal of Vibration and Acoustics* 120 (1998) 392–400.

[16] J. Greenstadt, Solution of wave propagation problems by the cell discretisation method, *Computer Methods in Applied Mechanics and Engineering* 174 (1999) 1–21.

[17] D.J. Nefske, S.H. Sung, Power flow finite element analysis of dynamic systems: basic theory and application of beams, *Journal of Vibration, Acoustics, Stress and Reliability in Design* 111 (1989) 94–100.

[18] A. Girard, H. Defosse, Frequency response smoothing and structural path analysis: application to beam trusses, *Journal of Sound and Vibration* 165 (1) (1993) 165–170.

[19] C. Soize, Medium frequency linear vibration of anisotropic elastic structures, *La Recherche Aérospatiale* 5 (1982) 65–87.

[20] E. De Langre, Fonctions de transfert de plaques en flexion par équation intégrales. Test de validation et de performance, rapport CEA: DMt/90/395, 1991.

[21] M. Ochmann, S.N. Makarov, An iterative solver of the Helmholtz integral equation for high frequency acoustic scattering, *Journal of the Acoustical Society of America* 103 (2) (1998) 742–750.

[22] C. Soize, Trends in modeling of structural acoustic systems with structural complexity in low and medium frequency range, *6ème International Congress on Acoustic* 4 (1998) 2423–2442.

[23] V.D. Belov, S.A. Ryback, Applicability of the transport equation in the one-dimensional wave propagation problem, *Akustiechbeskii Zhurnal Soviet Physics Acoutstics* 21 (2) (1975) 173–180.

[24] Y. Lase, M.N. Ichchou, L. Jéjéquel, Energy flow analysis of bars and beams: theoretical formulation, *Journal of Sound and Vibration* 192 (1) (1994) 2981–3005.

[25] A. Carcaterra, A. Sestiani, Energy density equation and power flow in structure, *Journal of Sound and Vibration* 188 (1995) 269–282.

[26] M.N. Ichchou, A. Le Bot, L. Jézéquel, A transient local energy approach as an alternative to transient SEA: wave and telegraph equations, *Journal of Sound and Vibration* 246 (2001) 829–840.

[27] P. Ladevèze, Prédiction des vibrations pour le calcul des vibrations moyennes fréquences, *NT Aérospatiale YX/SA* 116 471 (1995).

[28] R.S. Langley, On the vibrational conductivity approach to high frequency dynamics for two dimensional structural component, *Journal of Sound and Vibration* 182 (4) (1995) 637–657.

[29] P. Ladevèze, Une nouvelle approche pour le calcul des vibrations moyennes fréquences, *NT Aérospatiale YX/SA* 119 639 (1996).

[30] P. Ladevèze, L. Arnaud, P. Rouch, C. Blanzé, The variational theory of complex rays for the calculation of medium-frequency vibrations, *Engineering Computations* 18 (1/2) (2001) 193–214.

[31] W.T. Koiter, A consistent first approximation in the general theory of thin elastic shells, *Proceedings of the IUTM Symposium on Theory of Thin Elastic Shells*, Delft, August 1959, North-Holland, Amsterdam, 1960, pp. 12–33.

[32] W.T. Koiter, On the foundation of the linear theory of thin elastic shells, *Proceedings of the Koninklijke Nederlandse Akademie Van Wetenschapper* B73 (1970) 169–197.

[33] A.W. Leissa, *Vibration of shells*, Acoustical Society of America, New York, 1993.

[34] C.R. Steele, A geometric optics solution for the thin shell equations, *International Journal of Engineering Science* 9 (1970) 681–704.

[35] V.V. Bolotin, The edge effect in the oscillations of elastic shells, *Prikladnaya Matematika i Mekhanika* 24 (5) (1960) 831–843.

[36] B. Bouche, F. Molinet, Méthods asymptotiques en électromagnétisme, *Coll. Mathématiques et Applications*, Springer, Berlin.

[37] R. Ohayon, Local and global effects in the vibration of structures. A review synthesis, *ESTEC, ESA Workshop Proceeding on Modal Representation of Flexible Structures by Continuum Methods*, Noordwijk, Netherlands, 1989, pp. 29–54.

[38] L.L. Thompson, P.M. Pinsky, Complex wave number Fourier analysis of the p-version finite element method, *Computational Mechanics* 13 (1994) 255.